SCIENTIFIC REPORTS

SUBJECT AREAS:
NEUROSCIENCE
IMMUNOLOGY
INNATE IMMUNITY
VIROLOGY

Received
7 June 2012

Accepted
28 June 2012

Published
30 July 2012

Correspondence and requests for materials should be addressed to C.L.H. (howe@mayo.edu)

* Current address: Biosciential, Rochester, MN, USA.

Hippocampal protection in mice with an attenuated inflammatory monocyte response to acute CNS picornavirus infection

Charles L. Howe[1,2,3], Reghann G. LaFrance-Corey[1], Rhianna S. Sundsbak[1], Brian M. Sauer[1,4], Stephanie J. LaFrance[1], Eric J. Buenz[1]* & William F. Schmalstieg[1]

[1]Department of Neurology, College of Medicine, Mayo Clinic, Rochester, Minnesota, USA, 55905, [2]Department of Neuroscience, College of Medicine, Mayo Clinic, Rochester, Minnesota, USA, 55905, [3]Department of Immunology, College of Medicine, Mayo Clinic, Rochester, Minnesota, USA, 55905, [4]Medical Scientist Training Program, College of Medicine, Mayo Clinic, Rochester, Minnesota, USA, 55905.

Neuronal injury during acute viral infection of the brain is associated with the development of persistent cognitive deficits and seizures in humans. In C57BL/6 mice acutely infected with the Theiler's murine encephalomyelitis virus, hippocampal CA1 neurons are injured by a rapid innate immune response, resulting in profound memory deficits. In contrast, infected SJL and B6xSJL F1 hybrid mice exhibit essentially complete hippocampal and memory preservation. Analysis of brain-infiltrating leukocytes revealed that SJL mice mount a sharply attenuated inflammatory monocyte response as compared to B6 mice. Bone marrow transplantation experiments isolated the attenuation to the SJL immune system. Adoptive transfer of B6 inflammatory monocytes into acutely infected B6xSJL hosts converted these mice to a hippocampal damage phenotype and induced a cognitive deficit marked by failure to recognize a novel object. These findings show that inflammatory monocytes are the critical cellular mediator of hippocampal injury during acute picornavirus infection of the brain.

Immune control of acute infections in the CNS is uniquely constrained by the generally irreplaceable nature of neurons. The immune system must strike a balance between efficient control of the pathogen and protection of neural machinery in order to optimally maintain host survival and neurologic function[1]. The innate immune system is a necessary first responder to infection of the CNS that serves both to contain and constrain pathogen spread and to recruit elements of the adaptive immune response necessary to eradicate and permanently clear the pathogen from the host[2,3]. Chemokine expression by CNS-resident cells in response to pathogens triggers leukocyte adhesion to the cerebral vasculature[4–6], whereupon matrix metalloproteinases degrade the basal lamina of the blood-brain barrier[7], facilitating entry of the leukocytes into the brain parenchyma. The large numbers of circulating innate immune cells available to respond to infection coupled with the ability of these cells to rapidly produce and release antimicrobial and antiviral effector molecules[8] creates a double-edged sword. On the one hand, a robust innate immune response may be necessary to limit pathogen spread and promote the adaptive immune response[9]. On the other hand, a powerful but indiscriminate innate immune response may lead to substantial brain injury and subsequent death of the host[10].

We have previously shown that CA1 hippocampal pyramidal neurons die in C57BL/6 (B6) mice acutely infected with the Theiler's murine encephalomyelitis virus (TMEV) via a mechanism that involves oxidative injury, calpain and caspase activation, and ultimately apoptosis. Neuron death in our model is independent of direct cellular infection with the virus and precedes the adaptive immune response in the CNS[11,12]. We also recently determined that a rapid innate immune response to the acute infection is responsible for triggering a non-cell autonomous bystander pathology of hippocampal neurons[13]. In this previous study we found that depletion of both inflammatory monocytes and neutrophils but not neutrophils alone resulted in preservation of hippocampal neurons[13]. However, we were unable to explicitly reduce or remove only inflammatory monocytes without affecting neutrophils, weakening the direct relationship between monocytes and CA1 neuron injury. However, we have now identified SJL and B6xSJL F1 mice as strains that are resistant to hippocampal pathology during acute brain infection with TMEV and

we found that these animals mount an attenuated inflammatory monocyte response to the infection. Critically, the neutrophil response is not reduced. Moreover, adoptive transfer of B6-derived brain infiltration-competent inflammatory monocytes into acutely infected B6xSJL F1 mice recapitulated the B6-like hippocampal injury phenotype. Thus, here we provide further evidence that inflammatory monocytes are the key innate inflammatory effector responsible for the initiation of hippocampal neuron bystander immunopathology during acute picornavirus infection of the brain.

Results

Injury to CA1 hippocampal neurons associated with acute TMEV infection is absent in SJL mice despite robust infection with TMEV. We have previously characterized severe injury to CA1 hippocampal pyramidal neurons during acute infection of C57BL/6 (B6) mice with TMEV[12]. We showed that hippocampal injury was evident as early as 2 days postinfection (dpi) and continued to evolve such that by 7 dpi the majority of CA1 neurons were lost and cognitive performance was impaired[12]. During a screen for genetic models of susceptibility and resistance to this hippocampal injury we observed essentially complete preservation of CA1 neurons in the SJL strain. As shown in Figure 1, a substantial portion of CA1 neurons were lost in B6 mice by 4 dpi (Figure 1A; CA1 is region between arrowheads). By 21 dpi nearly all CA1 neurons were absent in B6 mice, as marked by Nissl histochemistry (Figure 1C) or NeuN immunostaining (Figure 1E). In contrast, most CA1 neurons were preserved in SJL mice at 4 dpi (Figure 1B) and this preservation persisted through 21 dpi (Figure 1D, 1F), indicating that the injury to CA1 was not simply delayed in SJL mice. In general, we only observed a small amount of CA1 neuronal loss in SJL mice, typically at the junction of the CA1 and CA3 regions of the pyramidal cell layer or sometimes near the midline. Higher resolution imaging (Figure 2) confirmed the extensive injury and loss of CA1 neurons at 4 dpi in B6 mice (Figure 2B) as compared to uninfected B6 controls (Figure 2A) and the retention of CA1 neurons in SJL mice at 4 dpi (Figure 2D; compare to uninfected SJL in Figure 2C). Of note, the large apical dendrites (arrowheads in Figure 2A–2F) projecting from the CA1 neurons were maintained in the infected SJL mice (Figure 2D) but not in the infected B6 mice (Figure 2B), despite the presence of inflammatory infiltrate in both strains (Figure 2B, 2D). The preservation effect is genetically dominant, as B6xSJL F1 offspring exhibit preservation of CA1 hippocampal neurons (Figure 2E, 2F). Quantitative assessment of CA1 hippocampal injury using an unbiased scoring system[11,12] (Figure 2G) indicated that the difference between B6 and SJL mice is highly significant ($H(2,37)=27.785$, $P<0.001$ by Kruskal-Wallis ANOVA on ranks; Dunn's pairwise comparison: B6 vs SJL, $P<0.05$; B6 vs B6xSJL F1, $P<0.05$; SJL vs B6xSJL F1, $P>0.05$).

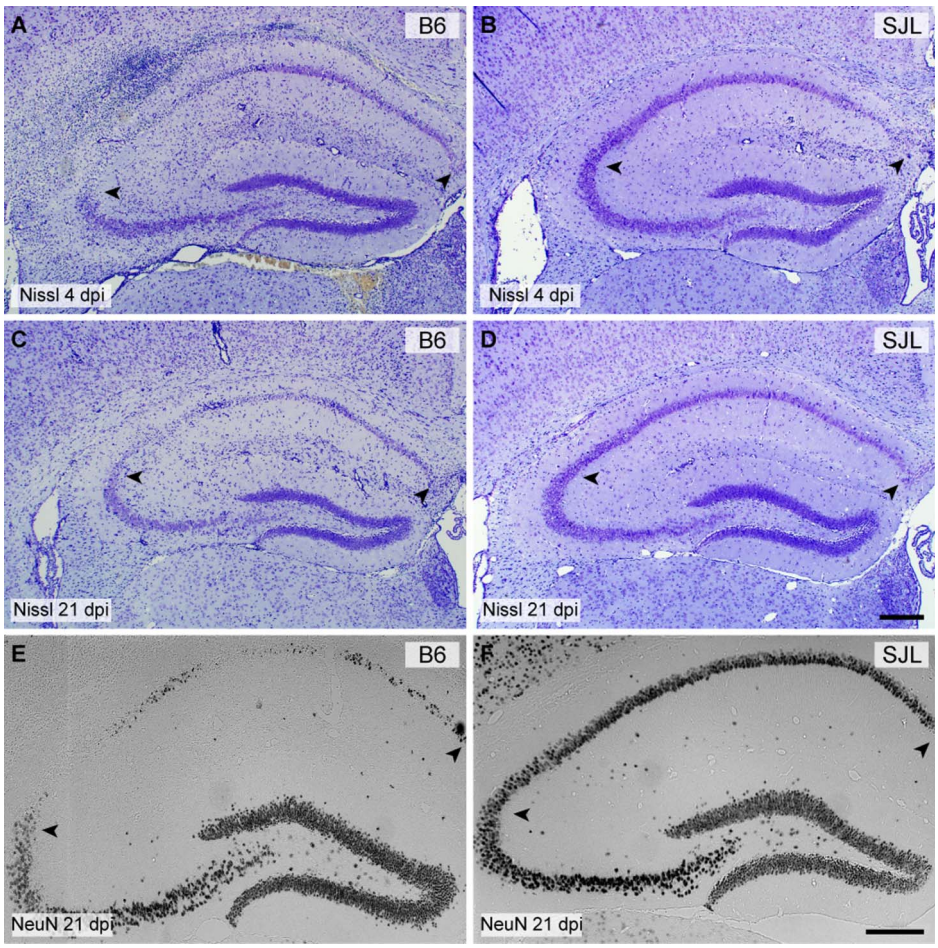

Figure 1 | Injury to CA1 hippocampal neurons associated with acute TMEV infection is absent in SJL mice. Hippocampal sections from B6 (A, C, E) and SJL (B, D, F) mice were processed for Nissl histochemistry (A–D) or immunostained for the neuron-specific marker NeuN (E–F) at 4 days postinfection (dpi) (A, B) or 21 dpi (C–F). By 4 dpi about 50% of CA1 region neurons are clearly lost in the B6 mouse (A) but minimal neuronal dropout is evident in the SJL mouse at this timepoint, despite the presence of a significant inflammatory response within the hippocampal fissure (B). By 21 dpi the majority of CA1 neurons are lost in B6 mice (C, E) while virtually all CA1 neurons are preserved in SJL mice (D, F). Scale bar in D is 250 μm and refers to A–C. Scale bar in F is 250 μm and refers to E. Arrowheads delineate the CA1 region. Sections are representative of at least 10 mice of each strain across multiple (>3) experiments.

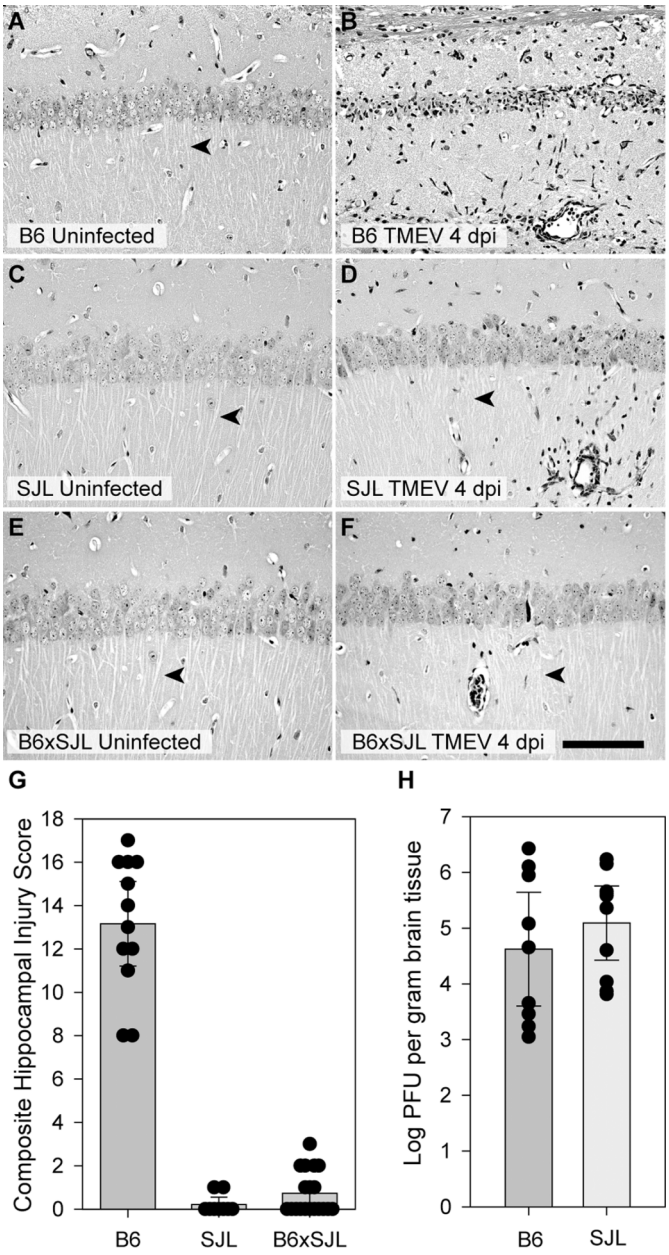

Figure 2 | Hippocampal protection during acute TMEV infection is genetically dominant and viral replication does not explain the protection of CA1 neurons in SJL mice. Hippocampal sections from uninfected (A, C, E) and 7 dpi (B, D, F) B6 (A, B), SJL (C,D), and B6xSJL F1 hybrids (E, F) were stained with hematoxylin and eosin. F1 hybrids, like the SJL parentals, do not exhibit substantial hippocampal injury. The extent of hippocampal injury was quantified (G) by summing the estimated percentage of CA1 neurons lost in each hemisphere represented on a scale of 0 to 10 (for example, the injury in Figure 1A is a 5). Zero indicates no injury to either hippocampus, while 20 represents complete loss of CA1 in both hemispheres. While there was no difference between SJL and F1 hybrid mice (B6xSJL), the injury observed in C57BL/6 mice was highly significant ($P<0.001$) compared to both groups. Viral load in the brain at 7 dpi was measured by standard plaque assay using brain homogenates incubated on L2 cells for 72 hours. (H) No difference was observed between B6 and SJL mice. Measurements for individual animals are shown in the scatter plots. The bar graphs represent the mean and 95% confidence intervals (95% CI) for the groups. Scale bar in F is 100 μm and refers to all panels. Sections are representative of at least 10 mice from each group in 3 separate experiments.

Strain-dependent differences in viral replication and viral persistence are a well-characterized aspect of TMEV infection[14]. It was therefore reasonable to hypothesize that SJL mice are protected from hippocampal injury due to lower viral titer or altered viral tropism in hippocampal neurons. However, plaque analysis of brain homogenate at 7 dpi (Figure 2H) revealed no difference in viral load between the strains ($t(1,17)= -0.900$, $P=0.381$ by t-test). In addition, there was no difference in viral load between strains at earlier timepoints (2, 3, 4 dpi) ($F(1,23)=1.287$, $P=0.273$ by two-way ANOVA). Likewise, the distribution of virus in the hippocampus did not differ between B6 (Figure 3A, 3E) and SJL (Figure 3B, 3F) mice at 3 dpi. Indeed, many healthy CA1 neurons in SJL mice exhibited robust infection, with virus antigen filling the large, intact apical dendrites of these cells (Figure 3F). In contrast, the apical dendrites of TMEV-immunoreactive CA1 neurons in B6 mice were already lost by 3 dpi (Figure 3E, 3G), indicating that these cells are injured. This observation supports our previous finding that hippocampal neuron apoptosis occurs independently of Theiler's virus in B6 mice[12]. We conclude that differences in viral replication or tropism do not account for the preservation of CA1 neurons in SJL mice.

Our previous observations regarding CA1 neuron loss during acute TMEV infection indicated that these neurons were dying apoptotically following an oxidative insult[12]. Therefore, a secondary hypothesis for the preservation of CA1 in SJL mice is that hippocampal neurons are less susceptible to apoptosis in this strain compared to B6 mice. Indeed, TUNEL staining at 5 dpi revealed that CA1 neurons were clearly undergoing apoptosis in B6 mice (Figure 4A) whereas essentially no TUNEL-positive CA1 hippocampal neurons were observed in SJL mice at 5 dpi (Figure 4B; based on known genetic defects in SJL mice, we speculate that the scattered TUNEL-positive cells are immune cells undergoing activation-induced cell death[15–17]). However, in vitro, hippocampal neurons derived from SJL mice were more sensitive to oxidative stress-induced cell death than B6 neurons as assessed using an MTT (3-(4,5-dimethylthiazol-2-yl)-2,5-diphenyltetrazolium bromide) assay (Figure 4C; $F(1,29)=8.556$, $P=0.009$ by two-way ANOVA; Student-Newman-Keuls pairwise comparison: B6 vs SJL at 3 mM H_2O_2, $P=0.019$; B6 vs SJL at 30 mM H_2O_2, $P=0.001$). Thus, we conclude that neurons from SJL mice are more or equally sensitive to apoptosis associated with oxidative injury, indicating that neuronal apoptotic resistance cannot explain the preservation phenotype observed in these animals.

The acute inflammatory monocyte response to TMEV infection is attenuated in SJL mice. Our previous observations regarding hippocampal injury in TMEV-infected B6 mice revealed a critical role for inflammatory monocytes in the death of CA1 neurons[13]. We found that inflammatory monocytes entered the brain as early as 6 hours post-infection (hpi) and peaked around 18 hpi. Immunodepletion of inflammatory monocytes and neutrophils but not neutrophils alone was sufficient to protect the hippocampus from injury[13]. Based on these observations we hypothesized that the preservation of the hippocampus observed at 7 dpi in SJL mice was due to a change in the acute inflammatory monocyte response mounted during the first 24 hpi. We therefore collected brain-infiltrating leukocytes (BILs) from B6 and SJL mice at 18 hpi and analyzed the cells by flow cytometry (Figure 5). We found a striking attenuation of the inflammatory monocyte response in SJL mice as compared to B6 mice. While the relative number of neutrophils ($CD45^{hi}CD11b^{++}Gr1^{+}1A8^{+}$) was increased in SJL mice (Figure 5D, 5F) compared to B6 (Figure 5C, 5E), the number of inflammatory monocytes ($CD45^{hi}CD11b^{+}Gr1^{+}1A8^{-}$) was sharply reduced in SJL mice (Figure 5D vs 5C, 5F vs 5E). Quantitation revealed that inflammatory monocytes in the SJL BILs were reduced to one-third of B6 levels (Figure 5G; $F(3,16)=183.427$, $P<0.001$ by two-way ANOVA; Student-Newman-Keuls pairwise comparison: B6 vs SJL monocytes, $P<0.001$; B6 vs SJL neutrophils, $P<0.001$). Because our

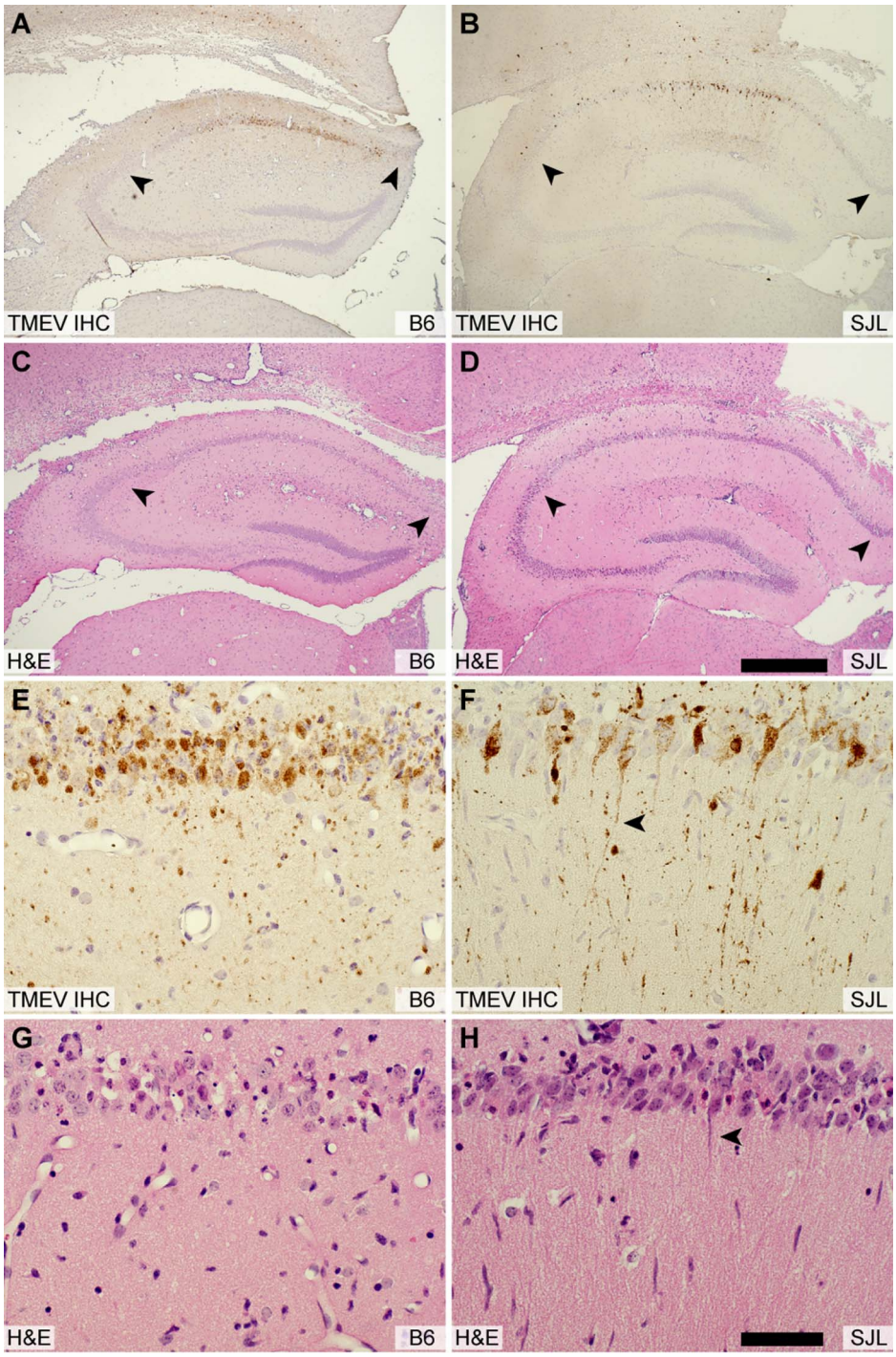

Figure 3 | Viral tropism does not explain the protection of CA1 neurons in SJL mice. Serial hippocampal sections from B6 (A, C, E, G) and SJL mice (B, D, F, H) were immunostained for the presence of virus (A, B, E, F) or were histologically stained with hematoxylin and eosin (C, D, G, H) at 3 dpi. This timepoint was chosen to represent the peak of viral replication in the CNS. Inspection of the low magnification pattern of anti-TMEV immunostaining reveals no difference in the tropism of the virus between strains (A, B). At higher magnification it is evident that SJL neurons are robustly infected (F) but have not experienced the same overt injury apparent in B6 mice (E). CA1 neurons in SJL mice exhibit normal apical dendrites (arrowhead in F and H) despite the presence of virus antigen extending throughout these dendrites. In contrast, CA1 neurons in B6 mice have already lost these dendrites by 3 dpi (E, G). The scale bar in D is 500 μm and refers to A–C. The scale bar in H is 50 μm and refers to E–G. Sections are representative of at least 3 mice per group in 3 separate experiments.

experiments utilized mixed sex groups, we separately analyzed male and female SJL mice to ensure that one sex was not dominating the response. Attenuation of the inflammatory monocyte response was observed in both male and female SJL mice relative to B6 mice ($F(3,13)=242.054$, $P<0.001$ by one-way ANOVA; Student-Newman-Keuls pairwise comparison: B6 male vs SJL male, $P<0.001$; B6 female vs SJL female, $P<0.001$; SJL male vs SJL female, $P=0.354$).

To further verify the observed attenuation of the inflammatory monocyte response in SJL mice, we employed a modified density gradient that results in enrichment of inflammatory monocyte yield and removal of neutrophils. In contrast to the 1.100 g/mL Percoll

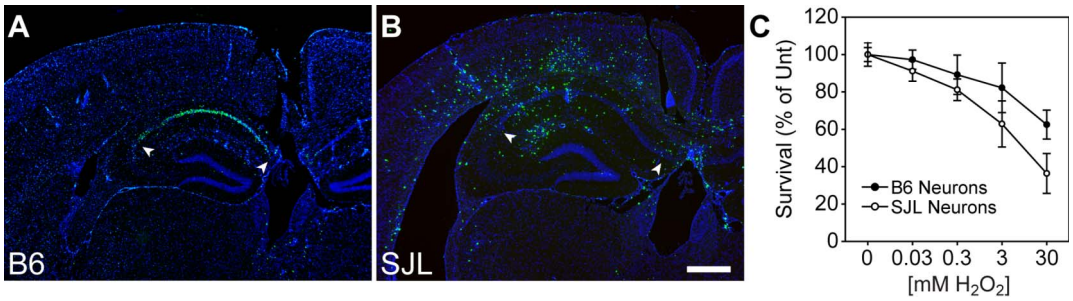

Figure 4 | CA1 neurons undergo apoptotic cell death in B6 mice but not in SJL mice during acute TMEV infection. Hippocampal sections from B6 (A) and SJL mice (B) were processed for TUNEL staining to mark apoptotic cells at 4 dpi. The majority of TUNEL-positive cells were localized to the CA1 pyramidal layer of the hippocampus in B6 mice (A), consistent with the observation that these neurons die within the first few days of infection. In contrast, very few TUNEL-positive cells were observed in the CA1 region of SJL mice (B), suggesting that neurons in the hippocampus do not die in these animals. The large number of TUNEL-positive cells scattered throughout the brain frequently colocalize with histological markers of inflammation. (C) Primary hippocampal neurons cultured from B6 mice (solid circle) and from SJL mice (empty circle) were exposed to various concentrations of H_2O_2 to determine sensitivity to oxidative injury-induced cell death using an MTT survival assay. Data are shown as percent of untreated MTT reaction product following spectrophotometric analysis of cell lysates. While there was a trend toward greater sensitivity to oxidative injury in neurons derived from SJL mice, this outcome is opposite to the prediction that increased neuron death in B6 mice is due to heightened sensitivity to apoptosis. The scale bar in B is 500 μm and refers to all panels. Sections are representative of at least 5 mice per group across multiple (>3) experiments.

interface used above, the modified gradient separated inflammatory monocytes from neutrophils at a 1.080 g/mL interface[18]. Using this gradient we again found a substantial difference in B6 BILs versus SJL BILs at 18 hpi that was even evident in the forward (FSC) and side scatter (SSC) plots (Figure 6A, 6B). While the total BILs yield was not different between the strains at two different timepoints (Figure 6G; $t(1,5) = -0.0518$, $P = 0.961$ by t-test at 18 hpi), the absolute number of $CD45^{hi}CD11b^{+}Gr1^{+}1A8^{-}$ inflammatory monocytes was reduced by 4-fold at 18 hpi and 3-fold at 24 hpi in SJL mice compared to B6 mice (Figure 6H, 6D vs 6C, 6F vs 6E; $t(1,5) = 19.659$, $P < 0.001$ by t-test at 18 hpi). We conclude that the acute inflammatory monocyte response to TMEV infection is highly attenuated in SJL mice.

Bone marrow transplantation reveals that the reduced inflammatory monocyte response in SJL mice is intrinsic to the immune system, not the CNS. We hypothesized that the attenuated SJL inflammatory monocyte response could arise either from a defective or reduced immune response (for example, reduced chemotropism or infiltration) or a defective or reduced brain response to the infection (for example, reduced chemokine production). To test this hypothesis we examined the extent of hippocampal injury in irradiated mice reconstituted with a heterologous immune system via bone marrow transplantation. In order to avoid MHC incompatibility issues we used C57BL/10SnSg (B10.S-H2s/SgMcdJ) mice ($H\text{-}2^{s}$ haplotype) for this analysis instead of B6 mice ($H\text{-}2^{b}$ haplotype). These mice, despite sharing the same MHC haplotype as SJL mice exhibited a robust inflammatory monocyte response and hippocampal injury comparable to B6 mice (see below). We used the differential expression of CD45.1 and CD45.2 on peripheral blood mononuclear cells to characterize the reconstitution of an SJL immune system ($CD45.2^{+}$) (Supplementary Figure 1C) in either SJL (controls) (Supplementary Figure 1G) or B10.S hosts (experimental) (Supplementary Figure 1F) versus reconstitution of a B10.S immune system ($CD45.1^{+}$) (Supplementary Figure 1D) in either B10.S (controls) (Supplementary Figure 1H) or SJL hosts (experimental) (Supplementary Figure 1E). Reconstitution with heterologous bone marrow was greater than 95% in all experiments. Eight weeks after bone marrow transplant, recipient mice were infected with TMEV.

Using the 1.080 g/mL gradient, we characterized the inflammatory monocyte response in the BILs population following bone marrow reconstitution (Figure 7A–E). At 18 hpi, there were fewer than 300 SJL inflammatory monocytes ($CD45.2^{hi}CD11b^{+}Gr1^{+}$) in the BILs isolated from either the SJL into B10.S transplants or the SJL into SJL transplants (Figure 7A, 7D, 7E) ($F(1,10) = 184.088$, $P < 0.001$ by two-way ANOVA for cell identity; $t(10) = 0.328$, $P = 0.747$ by Holm-Sidak pairwise comparison between SJL into B10.S and SJL into SJL). In contrast, there were approximately 2500 B10.S inflammatory monocytes ($CD45.1^{hi}CD11b^{+}Gr1^{+}$) in the BILs isolated from either the B10.S into SJL transplants or the B10.S into B10.S transplants (Figure 7A, 7B, 7C) ($t(10) = 2.444$, $P = 0.027$ (not significant; critical threshold = 0.025) by Holm-Sidak pairwise comparison between B10.S into SJL and B10.S into B10.S). The presence of 9-fold greater inflammatory monocytes in the mice reconstituted with B10.S bone marrow compared to mice reconstituted with SJL bone marrow was highly significant ($F(3,12) = 64.423$, $P < 0.001$ by two-way ANOVA for transplant phenotype; $t(12) = 13.568$, $P < 0.001$ by Holm-Sidak pairwise comparison between B10.S cells and SJL cells in the BILs population). We conclude that reconsitution of SJL mice with a B10.S immune system results in strong inflammatory monocyte infiltration into the brain during acute TMEV infection while reconstitution of B10.S mice with an SJL immune system converts these animals to a weakened inflammatory monocyte response phenotype. Of note, in these experiments the resident microglia maintained the recipient phenotype: 98.9±0.5% of microglia were SJL phenotype in the SJL mice reconstituted with B10.S bone marrow and 98.6±0.7% of microglia were B10.S phenotype in B10.S mice reconstituted with SJL bone marrow ($F(3,10) = 2.684$, $P = 0.103$ by one-way ANOVA). These findings suggest that the inflammatory monocyte reduction observed in SJL mice is due to a primary defect in the peripheral immune response to infection rather than a defect in neural-derived recruitment signals triggered by infection.

Based on our evidence that inflammatory monocyte infiltration is responsible for hippocampal injury, we predicted that SJL mice reconstituted with a B10.S immune system would exhibit loss of CA1 neurons while B10.S mice reconstituted with an SJL immune system would show hippocampal preservation. In control experiments, B10.S hosts reconstituted with a B10.S immune system (B10.S into B10.S) (Figure 7B) exhibited robust hippocampal injury (Figure 7F, 7J), while SJL hosts with a reconstituted SJL immune system (SJL into SJL) (Figure 7D) showed complete hippocampal preservation (Figure 7G, 7J), consistent with the phenotype observed in normal B10.S or SJL mice. In contrast, SJL hosts reconstituted with a B10.S-derived immune system (B10.S into SJL) (Figure 7C) exhibited extensive hippocampal injury that was indistinguishable from B10.S controls (Figure 7H, 7J; $F(3,36) = 40.681$, $P < 0.001$ by one-way ANOVA; $P = 0.235$, B10.S into SJL vs B10.S into B10.S; $P < 0.001$, B10.S into SJL vs SJL into SJL by Student-Newman-Keuls pairwise comparison). Likewise, B10.S hosts reconstituted with an SJL

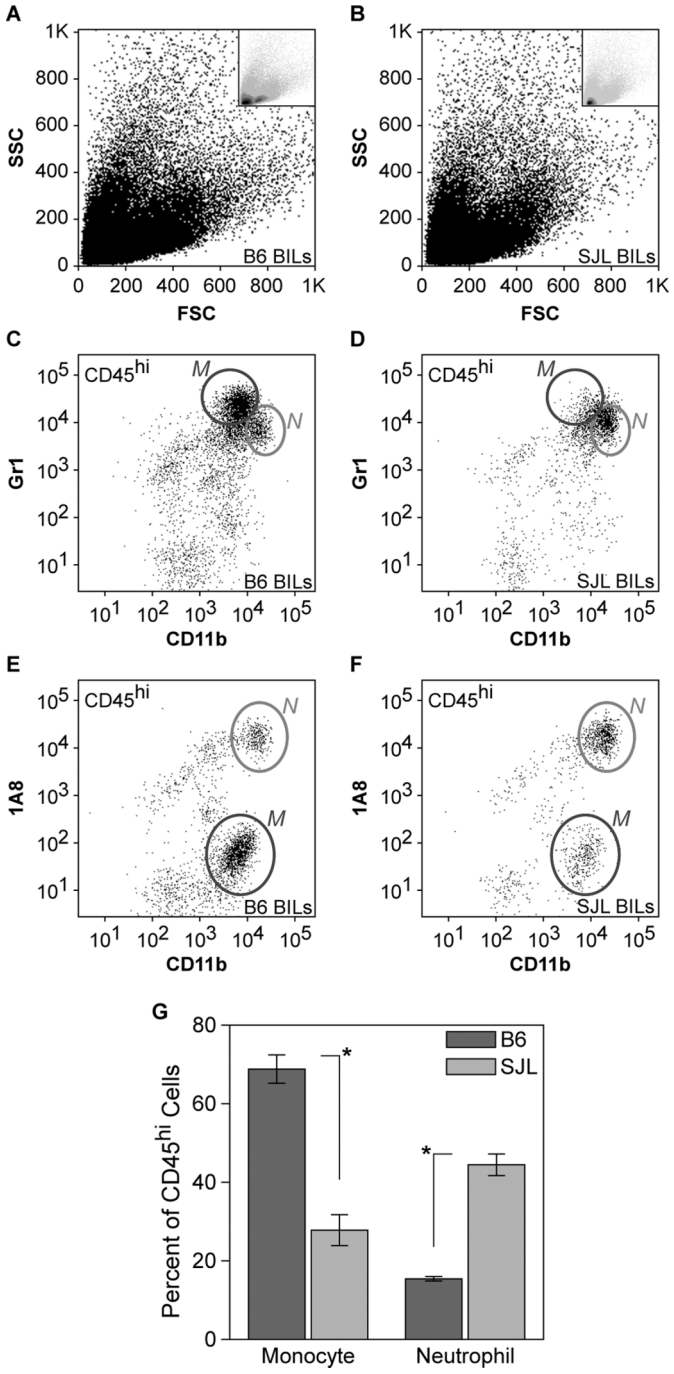

Figure 5 | Brain-infiltrating leukocytes differ between acutely infected B6 and SJL mice. Brain-infiltrating leukocytes (BILs) collected at 18 hours postinfection (hpi) using a 1.100 g/mL Percoll density gradient showed distinct forward scatter (FSC) and side scatter (SSC) profiles by flow cytometry in B6 mice (A) and SJL mice (B). Insets in A and B show density plots, highlighting the difference between B6 and SJL BILs. Gating on $CD45^{hi}$ cells revealed a clear difference in the number of $CD11b^{+}Gr1^{+}1A8^{-}$ inflammatory monocytes (labeled as *M*) in B6 mice (C, E) versus SJL mice (D, F). In contrast, the number of $CD11b^{++}Gr1^{+}1A8^{+}$ neutrophils (labeled as *N*) was slightly higher in SJL mice (D, F) than in B6 mice (C, E). The relative percent of $CD45^{hi}$ cells identified as inflammatory monocytes or neutrophils is shown in (G). The difference between B6 and SJL mice was highly significant, at $P<0.001$. Dot plots are representative of at least 4 animals per condition in at least 5 separate experiments. The error bars in (G) are centered on the mean percent of $CD45^{hi}$ BILs for the two gated populations and show the 95% CI for each group.

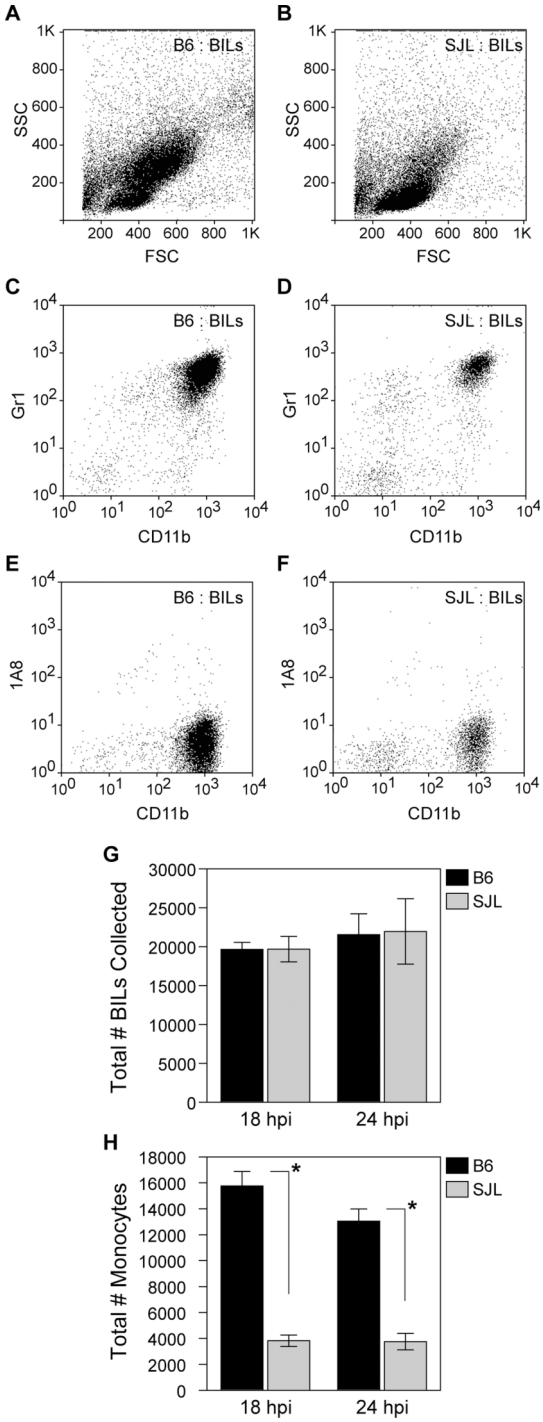

Figure 6 | Fewer inflammatory monocytes are recruited to the brain of acutely infected SJL mice as compared to B6 mice. B6 (A, C, E) and SJL (B, D, F) 18 hpi BILs were collected using a 1.080 g/mL Percoll gradient that removed the population of neutrophils while retaining inflammatory monocytes and analyzed by flow cytometry. FSC vs SSC plots revealed a large difference between B6 (A) and SJL mice (B). Gating on $CD45^{hi}$ cells showed that a large population of $CD11b^{+}Gr1^{+}1A8^{-}$ inflammatory monocytes was present in the B6 BILs at 18 hpi (C, E) and this population was substantially attenuated in SJL mice (D,F). While total BILs isolated from the two strains at either 18 or 24 hpi did not differ (G), the total number of inflammatory monocytes was greatly reduced in SJL mice at both timepoints (H). This difference was highly significant, at $P<0.001$ for both timepoints. The dot plots and quantitation are representative of at least 10 mice per condition in numerous experiments (>5). Graphs represent mean and 95% CI.

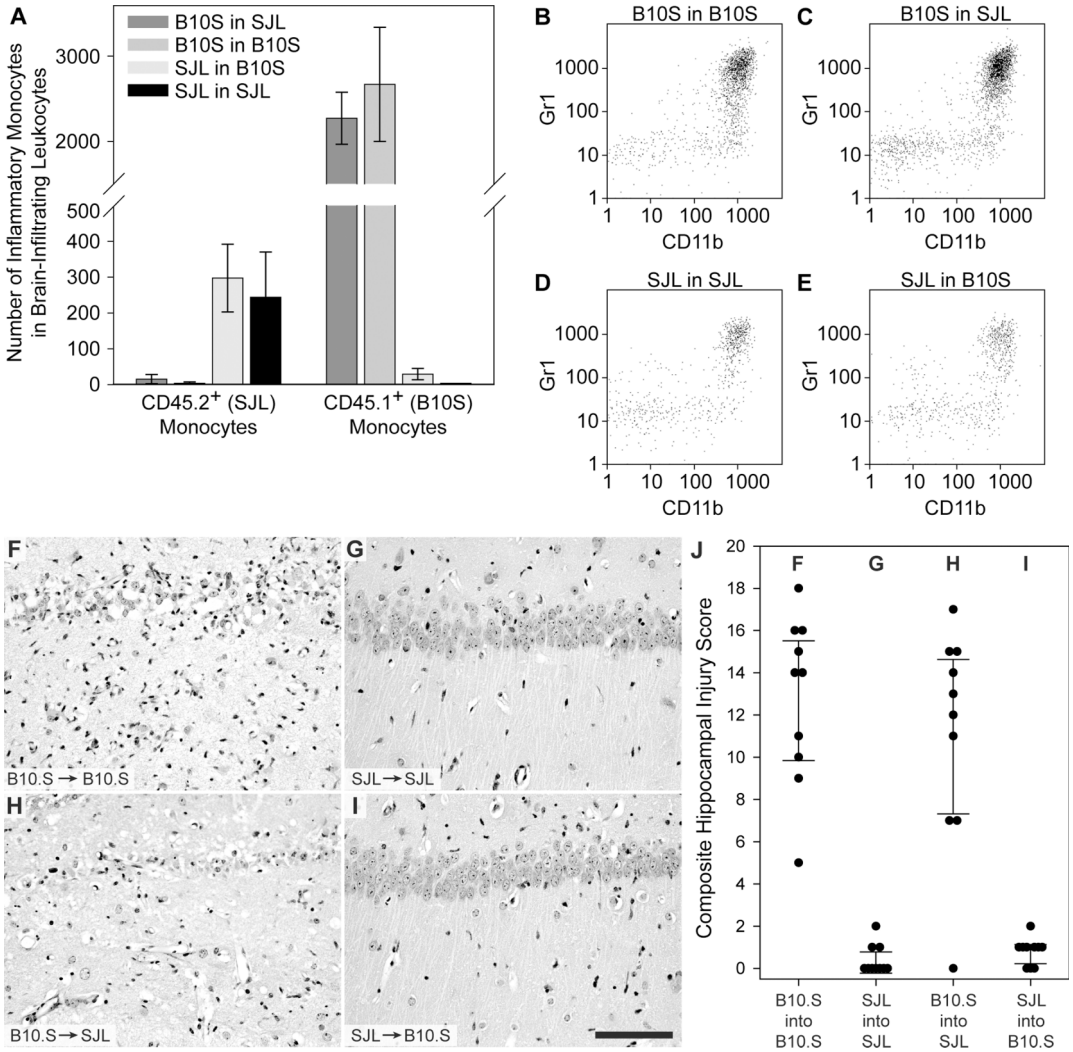

Figure 7 | Immune system identity predicts CA1 neuronal protection or injury. BILs were isolated using a 1.080 g/mL Percoll interface at 18 hpi from mice in the 4 bone marrow reconstitution groups described in Supplemental Figure 1 and phenotyped by flow cytometry. The number of SJL inflammatory monocytes ($CD45.2^+CD11b^+Gr1^+$) and B10.S inflammatory monocytes ($CD45.1^+CD11b^+Gr1^+$) were measured in each of the 4 transplant groups (A). SJL mice reconstituted with a B10.S immune system (C) had as many inflammatory monocytes as B10.S transplant controls (B), while B10.S mice reconstituted with an SJL immune system (E) exhibited the same low level inflammatory monocyte response observed in SJL transplant controls (D). Eight weeks after bone marrow reconstitution mice were infected with TMEV. Hippocampal sections were prepared at 7 dpi and injury to CA1 was quantified as in Figure 2. SJL mice reconstituted with a B10.S immune system (B10.S→SJL) (H) showed hippocampal damage that was indistinguishable from B10.S transplant controls (B10.S→B10.S) (F). Likewise, B10.S mice reconstituted with an SJL immune system (SJL→B10.S) (I) showed neuron preservation that was the same as SJL transplant controls (SJL→SJL) (G). Measurements for individual animals are shown in the scatter plot (J). Dot plots are representative of at least 4 mice in 2 separate experiments. The bar graph in A shows mean ± 95% CI. The error bars in J are centered on the mean hippocampal injury score and show the 95% CI for each group. The scale bar in I is 50 μm and refers to F–I. The pathology is representative of at least 10 mice per condition in 2 separate experiments.

immune system (SJL into B10.S) (Figure 7E) were completely protected and indistinguishable from SJL controls (Figure 7I, 7J; $P=0.786$, SJL into B10.S vs SJL into SJL; $P<0.001$, SJL into B10.S vs B10.S into B10.S by Student-Newman-Keuls pairwise comparison). We conclude that reconsitution of SJL mice with a B10.S immune system results in robust hippocampal injury during acute TMEV infection while reconstitution of B10.S mice with an SJL immune system converts these animals to a protected phenotype. This indicates that modulation of the inflammatory monocyte response (for example, conversion of the normally weak SJL response to a strong B10.S-type response) directly affects the extent of hippocampal injury (for example, conversion of the SJL protected phenotype to an injured phenotype based on the stronger B10.S inflammatory monocyte response).

Adoptive transfer of CNS infiltration-competent inflammatory monocytes reconstitutes hippocampal injury in SJL mice. Based on the bone marrow transplant results, we hypothesized that adoptive transfer of inflammatory monocytes into acutely infected SJL mice would result in hippocampal pathology. Due to a limited supply of B10.S donors we switched to the introduction of B6-derived cells into B6xSJL F1 hosts. As shown above, B6xSJL F1 mice exhibit the same hippocampal preservation phenotype as SJL mice during acute infection (Figure 2F, 2G). Because the host B6xSJL F1 mice are a mixed $H\text{-}2^{b/s}$ haplotype, introduction of $H\text{-}2^{b}$ donor leukocytes was not expected to trigger immune compatibility issues. We collected peritoneal exudates from uninfected B6 donors stimulated for 24 hr with mineral oil and isolated an inflammatory monocyte-enriched, neutrophil-deficient leukocyte population using

a 1.080 g/mL Percoll gradient (Figure 8A, 8B). Cells were adoptively transferred into B6xSJL F1 recipients at 18 hpi via tail vein injection. Six days after transfer (7 dpi) we found that B6xSJL F1 hosts receiving 10^6 peritoneal inflammatory monocytes exhibited severe hippocampal injury (Figure 8E, 8F, 8G), while infected B6xSJL F1 hosts receiving a sham adoptive transfer (PBS, no cells) (Figure 8C, 8G) and uninfected B6xSJL F1 hosts receiving 10^6 peritoneal inflammatory monocytes (Figure 8D, 8G) did not show hippocampal damage ($F(2,15)=107.478$, $P<0.001$ between all groups by one-way ANOVA; $t(2,15)=11.906$, $P<0.001$ between infected B6xSJL F1 hosts receiving inflammatory monocytes and infected B6xSJL F1 hosts receiving sham adoptive transfer by Holm-Sidak pairwise comparison). We conclude that the introduction of brain infiltration-competent B6 inflammatory monocytes into infected B6xSJL F1 hosts converted these mice to a hippocampal damage phenotype.

Finally, we tested the biological significance of the adoptive transfer induced hippocampal injury. We have previously correlated damage to hippocampal CA1 neurons with memory deficits in acutely infected B6 mice as assessed by Morris water maze and novel object recognition tests[11,12]. We employed a scent-based novel object recognition (NOR) test to assess memory performance following adoptive transfer of inflammatory monocytes into acutely infected B6xSJL F1 hosts. For this test, the ratio of time spent examining a novel scent object to the time spent examining a training scent object is taken as a discrimination index (DI)[12]. In mice with intact memory, the DI is always more than 1 and is frequently greater than 2, indicating that the mouse spends twice the time with the novel object as with the training object. As expected, based on the preservation of CA1 neurons in infected B6xSJL F1 mice, we found no significant loss of novel object recognition at 15 dpi in B6xSJL F1 hosts receiving sham adoptive transfers ($P=0.091$ with $q(10,100)=2.997$ by Student-Newman-Keuls pairwise comparison between B6xSJL F1 uninfected NOR DI and B6xSJL F1 15 dpi sham transfer NOR DI; $P=0.003$ with $q(10,100)=5.678$ by Student-Newman-Keuls pairwise comparison between B6xSJL F1 15 dpi sham transfer training DI and NOR DI; $F(9,100)=8.781$ by one-way ANOVA across all groups) (Figure 8H). In contrast, when inflammatory monocytes where adoptively transferred into acutely infected B6xSJL F1 hosts, we found that NOR was completely impaired at 15 dpi ($P=0.019$ with $q(10,100)=3.381$ by Student-Newman-Keuls pairwise comparison between B6xSJL F1 15 dpi sham transfer NOR DI and B6xSJL F1 15 dpi monocyte transfer NOR DI; $P=0.746$ with $q(10,100)=0.461$ by Student-Newman-Keuls pairwise comparison between B6xSJL F1 15 dpi monocyte transfer training DI and NOR DI) (Figure 8H). We conclude that the hippocampal damage caused by adoptively transferred inflammatory monocytes disrupts cognitive function in acutely infected SJL hosts.

Discussion

We recently hypothesized that neutrophils and inflammatory monocytes are important therapeutic targets for immunomodulatory or immunosuppressive therapies aimed at reducing or preventing CNS pathology associated with acute viral infection[13]. Kinetic analysis of leukocyte infiltration during the first 48 hours after TMEV infection revealed that inflammatory monocytes precede neutrophils, that both cell types are concentrated in the hippocampal formation, and that depletion of inflammatory monocytes and neutrophils but not neutrophils only resulted in preservation of the hippocampus and maintenance of cognitive performance[13]. In the present study we advance this previous work by providing additional evidence that inflammatory monocytes are a key mediator of hippocampal injury during acute picornavirus infection of the brain. We showed that despite comparable levels of virus infection and neutrophil infiltration between B6 and SJL mice, the hippocampus of SJL mice was essentially completely preserved. Critically, this preservation is apparently due to the reduced number of brain-infiltrating inflammatory monocytes in SJL mice, as reconstitution of a robust monocytic response via adoptive transfer results in hippocampal pathology that phenocopies B6 mice. In addition, using bone marrow transplantation, we showed that the attenuated inflammatory monocyte response in SJL mice was intrinsic to the immune cells, not the neural response to viral infection. While we do not know the genetic basis for this attenuated response, SJL mice do provide us with a naturally occuring model of a defective or attentuated (relative to B6 mice) inflammatory response to CNS infection. We interpret the current findings as very strong evidence that inflammatory monocytes are the critical mediator of hippocampal bystander pathology during acute picornavirus infection of the brain.

The mechanism of hippocampal injury mediated by infiltrating inflammatory monocytes is currently unclear. Inflammatory monocytes are a source of reactive oxygen species[19,20], blood-brain barrier (BBB)-degrading metalloproteinases[21–23], elastases[24], and cathepsins[25,26], as well as proinflammatory cytokines and chemokines[27,28]. Our previous observations indicate that CA1 neurons experience an oxidative injury that precedes the induction of calpain and caspase activation and the progression to apoptosis[12], suggesting that inflammatory monocytes create a toxic milieu within the hippocampus. Alternatively, inflammatory monocyte-mediated BBB disruption may trigger sufficient vascular permeability to induce seizures that ultimately destroy hippocampal neurons[29–31]. While the status of the BBB during acute TMEV infection remains to be tested, a generalized disruption of the BBB is difficult to reconcile with the apparent anatomic specificity for CA1 hippocampal injury associated with acute TMEV infection[12]. However, such specificity may arise from the sensitivity of hippocampal neurons to circuit disruption or to loss of homeostatic regulation of neurotransmitters and ions triggered by vascular leakage[32].

Fujinami and colleagues recently reported that TMEV-infected C57BL/6 mice develop seizures starting at around 3 dpi, while SJL and B6xSJL mice do not[33,34]. The absence of hippocampal pathology in SJL and B6xSJL mice in our current study corroborates this observation. In addition, Fujinami's group recently showed that behavioral seizures following TMEV infection were dependent upon innate immune responses but not the adaptive response[35,36]. These authors identified a critical role for inflammatory cytokines such as IL-6 and TNFα and proposed that innate effector cells responding to these cytokines were responsible for seizure induction. We now provide evidence that inflammatory monocytes may be sufficient to convert SJL mice to the hippocampal injury phenotype and are necessary to trigger hippocampal injury in C57BL/6 mice, perhaps via release of IL-6[37], TNFα[38,39], or other proinflammatory mediators. In support of this model, we have anecdotally observed that SJL mice receiving adoptive transfer of leukocytes from mineral oil-stimulated peritoneal exudate exhibit substantial seizures while C57BL/6 mice depleted of inflammatory monocytes do not seize at any point during the infection (data not shown). However, the cause-effect relationship between inflammatory monocytes, seizures, and hippocampal injury remains to be determined.

In addition to direct toxic effects or disruption of the BBB, brain-infiltrating inflammatory monocytes may produce chemokines that recruit additional effector cells such as neutrophils into the brain[40]. Based on work by Lane and colleagues using a neurotropic JHM strain of mouse hepatitis virus (JHMV) and antibody-mediated inhibition of CXCR2 signaling[41,42], one hypothesis for the role of acute inflammatory monocyte infiltration is that these cells influence entry of neutrophils into the brain that then modulate the adaptive immune response in a manner that determines whether TMEV persists or is cleared. This concept is further supported by observations in other viral models suggesting that monocytes are necessary for efficient T cell-mediated antiviral responses. For example, Bergmann and colleagues reported that monocytes mediate early access of antiviral T

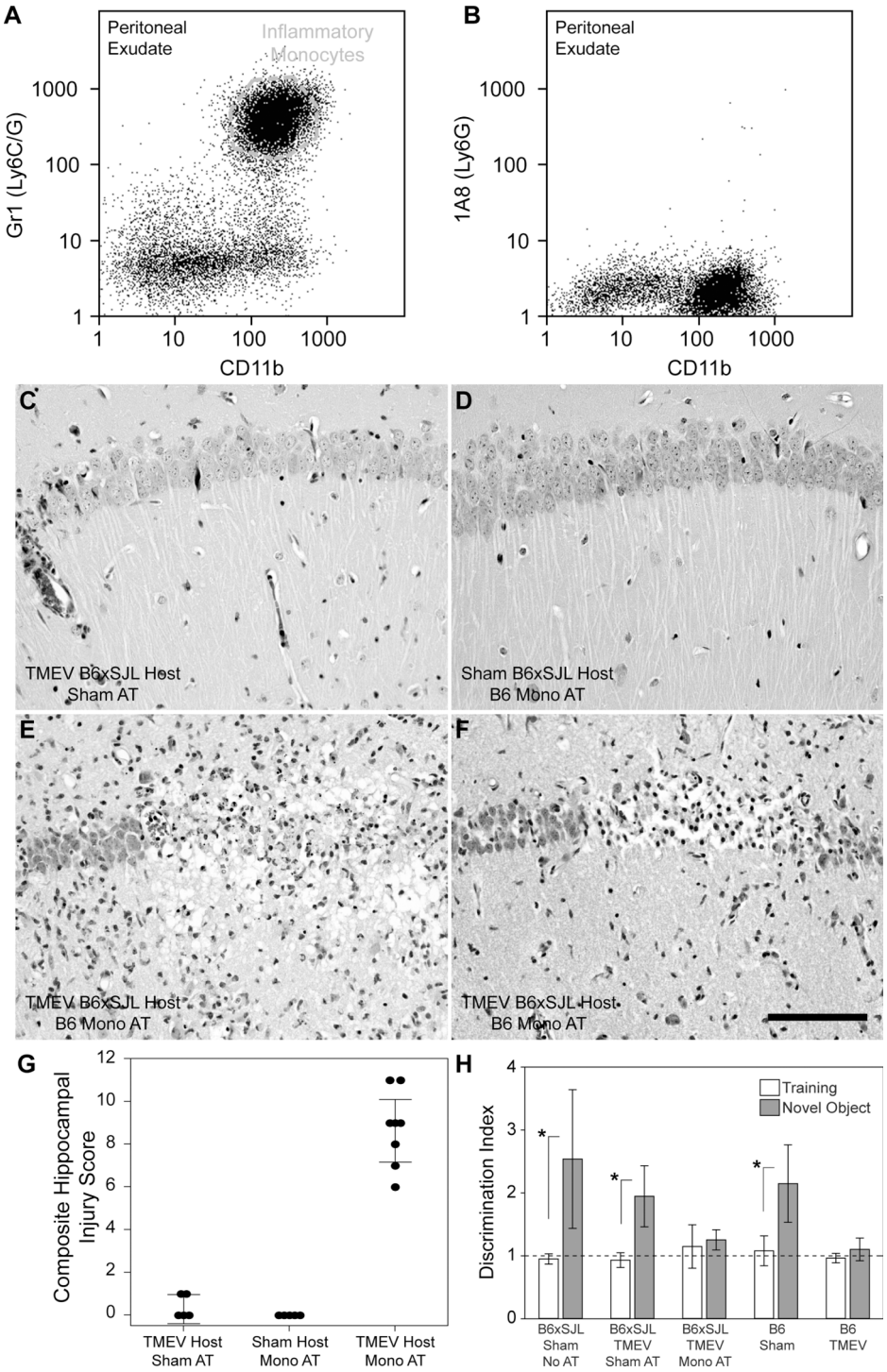

Figure 8 | Adoptive transfer of B6 inflammatory monocytes into acutely infected B6xSJL F1 mice results in hippocampal pathology and disruption of cognitive function. Inflammatory monocytes ($CD45^{hi}CD11b^{+}Gr1^{+}1A8^{-}$) collected at a 1.080 g/mL Percoll gradient from the peritoneal exudate of mineral oil-treated B6 mice (A, B) were adoptively transferred into B6xSJL F1 hosts and hippocampal pathology was assessed 6 days later (G). Infected B6xSJL F1 hosts that received a sham adoptive transfer (PBS, no cells) exhibited very little hippocampal injury (C). Likewise, uninfected B6xSJL F1 hosts that received 10^6 peritoneal inflammatory monocytes showed no evidence of hippocampal damage (D). In contrast, adoptive transfer of 10^6 peritoneal inflammatory monocytes into B6xSJL F1 hosts at 18–24 hpi caused considerable hippocampal injury (two representative animals shown in E and F). Cognitive performance was assessed following adoptive transfer (H). Infected B6xSJL F1 hosts were assessed in a novel object recognition test 14 days (equivalent to 15 dpi) after receiving an adoptive transfer of 10^6 peritoneal inflammatory monocytes ("Mono AT") or a sham adoptive transfer ("Sham AT"). The discrimination index (DI) represents the ratio of time spent investigating a novel object compared to a familiar object. A DI of 1 indicates equal time spent with both objects, indicating no memory for the familiar object. While cognitive function (memory of the familiar object) was preserved in the sham transfer B6xSJL F1 group (equivalent to uninfected B6xSJL F1 mice receiving no transfer and uninfected B6 mice), B6xSJL F1 mice receiving inflammatory monocytes by adoptive transfer exhibited the same loss of test performance observed in B6 mice at 15 dpi (B6 TMEV). Scale bar in F is 100 μm and refers to C–F. The pathology is representative of at least 5 mice per condition in 3 separate experiments. The error bars in G are centered on the mean hippocampal injury score and show the 95% CI for each group. The error bars in H are centered on the mean discrimination index and show 95% CI. The dashed line in H shows a DI equivalent to no recognition of the novel object.

cells into the parenchyma of JHMV-infected mice[9]. Using CCL2-deficient mice, these investigators showed that viral clearance is delayed by the absence of monocytes, apparently via a reduction in glia limitans disruption that caused retention of other leukocytes in the perivascular space. While we did not assess viral clearance or the kinetics of chronic disease development in our experiments, it is interesting that neither the low inflammatory monocyte-responding SJL mice nor inflammatory monocyte-depleted C57BL/6 mice experience an overwhelming and fatal viral infection. Instead, counterintuitively, the absence of an inflammatory monocyte response protected the hippocampus and preserved cognitive function, begging the question: what is the role for these cells in the most hyperacute response to viral infection of the brain?

A simplistic model for the relevance of this injury to host preservation and viral clearance would posit that the innate immune response limits viral spread and sacrifices hippocampal integrity in exchange for host survival. However, such a model fails to explain why hippocampal neurons that aren't infected are killed, why neurons that are infected in other regions of the brain survive, and why SJL mice experience robust viral infection of hippocampal neurons yet go on to clear the virus from the brain[12,43,44]. Indeed, our current behavioral analyses suggest that at least from a cognitive standpoint, the failure of inflammatory monocytes to enter the CNS in SJL mice is a protective phenotype. This is unexpected, given the normal distinction between C57BL/6 mice as a "resistant" strain and SJL mice as a "susceptible" strain[45,46]. While it is unlikely that the host resistance phenotype is determined by the acute inflammatory monocyte response, especially given the known genetics of resistance[46,47], it is intriguing that Fujinami observed an absence of seizures in three mouse strains that clear TMEV from the brain but not from the spinal cord[33]. However, the ultimate relationship between innate immune system-mediated bystander pathology in the hippocampus and the eventual clearance of virus from the host has yet to be fully explored.

The relationship between monocytes and other leukocytes in the control of immune system access to the brain parenchyma is likely far more complicated than previously suspected[2,48–52], and the role of these populations in acute control of TMEV infection is unknown. We are currently assessing the interaction of brain-infiltrating inflammatory monocytes, macrophages, and neutrophils during the most acute response to TMEV infection, the role these cells may play in seizure induction and epileptogenesis, and the impact of the acute inflammatory response on viral control and clearance. While many questions remain to be resolved, our current observations and recent findings[13] clearly indicate that inflammatory monocytes are a key mediator of hippocampal injury during acute picornavirus infection of the CNS.

Methods

Mice. C57BL/6/J (#000664), SJL/J (#000686), and C57BL/10SnSg (B10.S-H2s/SgMcdJ) (#001953) mice were acquired from The Jackson Laboratories (Bar Harbor, ME). Mice were acclimatized for at least one week following shipment prior to use. F1 hybrids from C57BL/6 and SJL parents were generated in our facility. Mice were group housed in the Mayo Clinic research vivarium under conventional conditions with ad libitum access to food and water. Sex was mixed for all experiments. All animal experiments conformed to the National Institutes of Health guidelines. All experiments were approved by the Mayo Clinic Institutional Animal Care and Use Committee.

Virus. At 5–6 weeks of age, mice were infected by intracranial injection of 2×10^5 PFU of the Daniel's strain of the Theiler's murine encephalomyelitis virus (TMEV) in 10 μL DMEM (the media used to grow the virus). When relevant, sham-infected mice received intracranial injection of 10 μL virus-free DMEM.

Histology, pathology, virus antigen staining, NeuN staining and TUNEL. Following intraperitoneal injection of a terminal dose of pentobarbital (100 mg/kg), mice were perfused via intracardiac puncture with 50 mL of 4% paraformaldehyde in PBS. The brain was postfixed in 4% paraformaldehyde at 4°C for 6 hr and then sectioned via coronal cuts at the level of the optic chiasm and infundibulum. Tissue blocks were embedded in paraffin, sectioned at 5 microns, mounted on charged slides, rehydrated, and stained with hematoxylin and eosin or with Nissl. Damage to the CA1 pyramidal neuron layer of the hippocampus was scored as previously described[12]. NeuN and virus antigen staining and the TUNEL reaction were performed as previously described[12].

Plaque assay. Viral titers were measured in brain homogenates at 7 dpi following our previously published protocol[53]. Briefly, a 10% (wt/vol) homogenate was prepared in DMEM, sonicated 3 times for 20 s each, clarified by centrifugation, and stored at −80°C until use. Confluent monolayers of L2 fibroblasts (ATCC: CCL-149) grown in DMEM containing 10% FBS were washed once with serum-free DMEM and then adsorbed with 10-fold dilutions (100–1010) of tissue homogenate prepared in 200 μL serum-free DMEM for 1 hr at 37°C. Without washing, cells were overlaid with 1 mL of 1% SeaPlaque agarose prepared in DMEM containing 2% FBS and HEPES. After solidifying at RT for 10 min, plates were incubated for 72 hr at 37°C. Cells and agarose plugs were fixed in EtOH:HOAc:formaldehyde (6 : 2 : 1) for 1 hr at RT. After gentle removal of the agarose, plates were washed in water, stained for 5 min in 1% crystal violet prepared in 20% EtOH, washed extensively with running water, and then dried. Plaques were counted in triplicate at 3 readable dilutions and back-calculated to give PFU/mL tissue homogenate.

Hippocampal neuron preparation. Primary cultures of hippocampal neurons were prepared from embryonic day 17 (E17) C57BL/6 or SJL mouse pups. Neurons were grown for 10–12 days before treatment. Briefly, hippocampi were collected in Hank's buffered salt solution (HBSS) containing 10 mM HEPES. Tissues were digested for 10–15 min in HBSS containing papain (1 mg/mL) and then allowed to settle. The supernatant (containing papain) was removed and the tissue was gently triturated in DMEM containing 10% FCS with a fire-polished Pasteur pipette to dissociate larger aggregates and stop papain activity. Cells were centrifuged for 5 min at 300 g and the cell pellet was resuspended in media. Neurons were then counted, seeded on poly-D-ornithine-coated coverslips in 12-well plates at a density of 2×10^5 cells/mL, and cultured in DMEM:F12 containing 10% FCS for 24 hours. After cells attached to the substrate, media was replaced with Neurobasal-A supplemented with B27, followed by re-incubation for 7–10 days, with half the medium replaced every 3 days.

In vitro induction of apoptosis. Hippocampal neurons were exposed to hydrogen peroxide (0 to 30 mM) for 24 hr at 37°C to induce apoptosis. During the final hour of incubation, 0.5 mg of 3-[4,5-dimethylthiazol-2-yl]-2,5-diphenyltetrazolium bromide (MTT) was added to the media without disturbing the cell layer. Viability was assessed by aspirating the media, lysing the cells in 1 mL SDS:DMF (50 : 50) for 15 min at RT, clarifying the lysate, and reading absorbance at 570 nm. Percent viability was calculated by normalizing to A570 in untreated cultures.

Bone marrow transplantation. Hosts for bone marrow reconstitution were treated with 0.12 g/L tetracycline HCl in drinking water for 1 week prior to irradiation with 900 rads over 10 min in a ^{137}Cs irradiator. Donor mice were killed by isoflurane overdose and bone marrow was flushed with ice-cold PBS from both femurs and tibias. Following trituration through a 27 G needle, bone marrow was strained at 30 μm via gravity, washed, resuspended in ACK buffer (155 mM NH4Cl, 10 mM KHCO3, 0.01 mM EDTA in water) to lyse red blood cells, washed in RPMI containing 10% FCS, and counted using trypan blue exclusion. Irradiated recipients received 10^7 bone marrow cells via tail vein injection. Reconstitution proceeded for 8 weeks prior to experimental use.

Isolation of brain-infiltrating leukocytes (BILs). BILs were prepared following our published protocol with slight modification[18]. Leukocytes were extracted from dounce homogenized brain tissue by centrifugation through a 30% Percoll gradient at 7800 g_{ave} for 30 min at RT in a Beckman F0630 rotor. After centrifugation the myelin debris layer that floated at the top of the gradient was removed by aspiration and the leukocyte layer floating just above the red blood cell pellet was collected, strained at 40 μm via gravity, diluted to 50 mL in PBS, and centrifuged at 1500 rpm (600 g_{ave}) for 5 min at RT in a clinical centrifuge to collect the cell pellet. The leukocyte pellet was resuspended in 1 mL PBS and underlaid with 1 mL of either 1.080 g/mL Percoll (monocyte enrichment) or 1.100 g/mL Percoll (monocytes and neutrophils). Following centrifugation at 800 g for 20 min at RT in a clinical centrifuge with no brake, the mononuclear leukocytes were collected at the gradient interface, washed in PBS, and resuspended in flow cytometry blocking buffer for analysis.

Flow cytometry. For all experiments, flow cytometry buffer contained 1% bovine serum albumin and 0.02% sodium azide in PBS. Blocking buffer contained flow cytometry buffer, supernatant from 2.4G2 hybridoma (Fc block; anti-CD16/32; ATCC, Manassas, VA, No. HB-197), and fetal bovine serum at a ratio of 10 : 5 : 1. After isolation, cells were suspended in blocking buffer and incubated at 4°C for 30 minutes. Antibodies were added to the blocked cells at 1 : 200 and incubated for 30 minutes at 4°C. Stained cells were then washed three times in flow cytometry buffer and fixed in 2% paraformaldehyde prior to flow cytometric analysis. Files were analyzed offline using FlowJo 7.5 (Windows version; Tree Star, Inc., Ashland, OR). CD45 was detected with clone 30-F11 (BD Biosciences No. 557235). CD11b was detected with clone M1/70 (BD Biosciences No. 553312). Ly6C/G was detected with clone Gr1, RB6-8C5 (BD Biosciences No. 553128). Ly6G was detected with clone 1A8 (BD Biosciences No.560599). CD45.1 was detected with clone A20 (BD Biosciences 553776). CD45.2 was detected with clone 104 (BD Biosciences No. 553772).

Flow cytometric phenotyping. Based on our previously published observations[13], we gated all brain-infiltrating cells on $CD45^{hi}$ expression. This gated population was subsequently assessed for expression of CD11b, Ly6C/G (Gr1), and Ly6G (1A8). We defined inflammatory monocytes as $CD45^{hi}CD11b^{+}Gr1^{+}1A8^{-}$ cells and neutrophils as $CD45^{hi}CD11b^{++}Gr1^{+}1A8^{+}$ cells. Note that microglia, defined as $CD45^{mid}CD11b^{mid}Gr1^{-}1A8^{-}$ were excluded from most analyses and are not shown in the flow plots. In experiments involving bone marrow chimeric mice, BILs were first gated on $CD45^{hi}$ expression, then phenotyped by CD11b, Gr1, and 1A8 expression; the inflammatory monocyte population was then assessed for expression of CD45.1 (B10.S marker) or CD45.2 (SJL marker).

Adoptive transfer of peritoneal exudate-derived leukocytes. Peritoneal leukocytes were elicited by intraperitoneal injections of 1 mL sterile mineral oil at 24 hr prior to collection. Cells were collected by peritoneal lavage with 10 mL sterile PBS, washed, and isolated from a discontinuous percoll gradient layer (1.080 g/mL interface). Prior to adoptive transfer, mice were handled daily for 5 minutes and inserted into a restraint device used for tail vein injections in order to decrease stress response. Host mice were infected with TMEV 18 hours prior to transfer, and 10^6 donor leukocytes were transferred via tail vein injection. Shams received PBS by tail vein injection.

Novel object recognition test. We followed our previously published protocol[12]. In brief, individual mice were tested using a 5 min habituation, 1 min rest, 10 min training, 5 min rest, 10 min testing paradigm. Training and testing objects were apple-, berry-, or cherry-scented tea candles arranged in diametric quadrants of an activity box. The scented candles were not treated as food. The novel object recognition testing session consisted of a 10 min exposure to one control object (same object and scent from the training session) and one novel scent object (randomly assigned scent not present in the training session; quadrant location for the novel object was also randomized between trials but diametric positioning was maintained). The number of interrogations of the novel object was divided by the number of investigations of the control object to generate a discrimination index (DI). Intact recognition memory produces a DI of 1 for the training session and a DI greater than 1 for the testing session, consistent with greater interrogation of the novel object. We routinely observed DI values greater than 2 for the testing session in normal mice.

Statistical analysis. $\alpha=0.05$ and $\beta=0.2$ were established a priori. Post hoc power analysis was performed for all experiments and significance was only considered when power$\geq$0.8. Statistical analysis was performed using the SigmaStat component of SigmaPlot (Systat Software, Inc; San Jose, CA). The Shapiro-Wilk test was applied to all data to determine normality[54]. Normally distributed data were then analyzed for equal variance. Data were only analyzed with parametric tests if both normality and equal variance were established. The Holm-Sidak or Student-Newman-Keuls pairwise comparison tests were used for all post hoc sequential comparisons[55]. Statistical values are reported following Curran-Everett guidelines[56]. The t-test was applied to the analysis of viral titer. One-way ANOVA was applied to the flow cytometric analysis of BILs between strains, measurement of hippocampal injury following bone marrow transplant or adoptive transfer, and to the novel object recognition analysis. Two-way ANOVA was used for the analysis of brain-infiltrating leukocytes in the bone marrow transplant experiments and in the MTT assay of hippocampal neuron death. The only non-parametric data were acquired during measurement of hippocampal injury between C57BL/6, SJL, and B6xSJL F1 mice; these data were analyzed with the Kruskal-Wallis one-way ANOVA on ranks test[57] using Dunn's pairwise comparison[58]. All graphs represent mean $\pm$ 95% confidence intervals.

1. Wilson, E. H., Weninger, W. & Hunter, C. A. Trafficking of immune cells in the central nervous system. *J Clin Invest* **120**, 1368–1379 (2010).
2. Silva, M. T. Neutrophils and macrophages work in concert as inducers and effectors of adaptive immunity against extracellular and intracellular microbial pathogens. *J Leukoc Biol* **87**, 805–813 (2010).
3. Savarin, C. & Bergmann, C. C. Neuroimmunology of central nervous system viral infections: the cells, molecules and mechanisms involved. *Curr Opin Pharmacol* **8**, 472–479 (2008).
4. Prinz, M. & Priller, J. Tickets to the brain: role of CCR2 and CX3CR1 in myeloid cell entry in the CNS. *J Neuroimmunol* **224**, 80–84 (2010).
5. Ransohoff, R. M. Chemokines and chemokine receptors: standing at the crossroads of immunobiology and neurobiology. *Immunity* **31**, 711–721 (2009).
6. Rot, A. & von Andrian, U. H. Chemokines in innate and adaptive host defense: basic chemokinese grammar for immune cells. *Annu Rev Immunol* **22**, 891–928 (2004).
7. Rosenberg, G. A. Matrix metalloproteinases in neuroinflammation. *Glia* **39**, 279–291 (2002).
8. Dale, D. C., Boxer, L. & Liles, W. C. The phagocytes: neutrophils and monocytes. *Blood* **112**, 935–945 (2008).
9. Savarin, C., Stohlman, S. A., Atkinson, R., Ransohoff, R. M. & Bergmann, C. C. Monocytes regulate T cell migration through the glia limitans during acute viral encephalitis. *J Virol* **84**, 4878–4888 (2010).
10. Kim, J. V., Kang, S. S., Dustin, M. L. & McGavern, D. B. Myelomonocytic cell recruitment causes fatal CNS vascular injury during acute viral meningitis. *Nature* **457**, 191–195 (2009).
11. Buenz, E. J., Rodriguez, M. & Howe, C. L. Disrupted spatial memory is a consequence of picornavirus infection. *Neurobiol Dis* **24**, 266–273 (2006).
12. Buenz, E. J. *et al.* Apoptosis of Hippocampal Pyramidal Neurons Is Virus Independent in a Mouse Model of Acute Neurovirulent Picornavirus Infection. *Am J Pathol* **175**, 668–684 (2009).
13. Howe, C. L., Lafrance-Corey, R. G., Sundsbak, R. S. & Lafrance, S. J. Inflammatory monocytes damage the hippocampus during acute picornavirus infection of the brain. *J Neuroinflammation* **9**, 50 (2012).
14. Brahic, M., Bureau, J. F. & Michiels, T. The genetics of the persistent infection and demyelinating disease caused by Theiler's virus. *Annu Rev Microbiol* **59**, 279–298 (2005).
15. Schlitt, B. P., Felrice, M., Jelachich, M. L. & Lipton, H. L. Apoptotic cells, including macrophages, are prominent in Theiler's virus-induced inflammatory, demyelinating lesions. *J Virol* **77**, 4383–4388 (2003).
16. Tsunoda, I., Libbey, J. E., Kuang, L. Q., Terry, E. J. & Fujinami, R. S. Massive apoptosis in lymphoid organs in animal models for primary and secondary progressive multiple sclerosis. *Am J Pathol* **167**, 1631–1646 (2005).
17. Suvannavejh, G. C., Dal Canto, M. C., Matis, L. A. & Miller, S. D. Fas-mediated apoptosis in clinical remissions of relapsing experimental autoimmune encephalomyelitis. *J Clin Invest* **105**, 223–231 (2000).
18. Lafrance-Corey, R. G. & Howe, C. L. Isolation of Brain-infiltrating Leukocytes. *J Vis Exp* **52**, 2747 (2011).
19. Fang, F. C. Antimicrobial reactive oxygen and nitrogen species: concepts and controversies. *Nat Rev Microbiol* **2**, 820–832 (2004).
20. Weiss, S. J., King, G. W. & LoBuglio, A. F. Evidence for hydroxyl radical generation by human Monocytes. *J Clin Invest* **60**, 370–373 (1977).
21. Malik, N., Greenfield, B. W., Wahl, A. F. & Kiener, P. A. Activation of human monocytes through CD40 induces matrix metalloproteinases. *J Immunol* **156**, 3952–3960 (1996).
22. Welgus, H. G. *et al.* Neutral metalloproteinases produced by human mononuclear phagocytes. Enzyme profile, regulation, and expression during cellular development. *J Clin Invest* **86**, 1496–1502 (1990).
23. Zhang, H. *et al.* Matrix metalloproteinase-9 and stromal cell-derived factor-1 act synergistically to support migration of blood-borne monocytes into the injured spinal cord. *J Neurosci* **31**, 15894–15903 (2011).
24. Xie, D. L., Meyers, R. & Homandberg, G. A. Release of elastase from monocytes adherent to a fibronectin-gelatin surface. *Blood* **81**, 186–192 (1993).
25. Reddy, V. Y., Zhang, Q. Y. & Weiss, S. J. Pericellular mobilization of the tissue-destructive cysteine proteinases, cathepsins B, L, and S, by human monocyte-derived macrophages. *Proc Natl Acad Sci U S A* **92**, 3849–3853 (1995).
26. Rossman, M. D., Maida, B. T. & Douglas, S. D. Monocyte-derived macrophage and alveolar macrophage fibronectin production and cathepsin D activity. *Cell Immunol* **126**, 268–277 (1990).
27. Liddiard, K., Rosas, M., Davies, L. C., Jones, S. A. & Taylor, P. R. Macrophage heterogeneity and acute inflammation. *Eur J Immunol* **41**, 2503–2508 (2011).
28. Serbina, N. V., Jia, T., Hohl, T. M. & Pamer, E. G. Monocyte-mediated defense against microbial pathogens. *Annu Rev Immunol* **26**, 421–452 (2008).
29. Marchi, N. *et al.* Seizure-promoting effect of blood-brain barrier disruption. *Epilepsia* **48**, 732–742 (2007).
30. Oby, E. & Janigro, D. The blood-brain barrier and epilepsy. *Epilepsia* **47**, 1761–1774 (2006).
31. Seiffert, E. *et al.* Lasting blood-brain barrier disruption induces epileptic focus in the rat somatosensory cortex. *J Neurosci* **24**, 7829–7836 (2004).
32. David, Y. *et al.* Astrocytic dysfunction in epileptogenesis: consequence of altered potassium and glutamate homeostasis? *J Neurosci* **29**, 10588–10599 (2009).
33. Libbey, J. E. *et al.* Seizures following picornavirus infection. *Epilepsia* **49**, 1066–1074 (2008).
34. Stewart, K. A., Wilcox, K. S., Fujinami, R. S. & White, H. S. Development of postinfection epilepsy after Theiler's virus infection of C57BL/6 mice. *J Neuropathol Exp Neurol* **69**, 1210–1219 (2010).
35. Kirkman, N. J., Libbey, J. E., Wilcox, K. S., White, H. S. & Fujinami, R. S. Innate but not adaptive immune responses contribute to behavioral seizures following viral infection. *Epilepsia* **51**, 454–464 (2010).
36. Libbey, J. E., Kennett, N. J., Wilcox, K. S., White, H. S. & Fujinami, R. S. Interleukin-6, produced by resident cells of the central nervous system and infiltrating cells, contributes to the development of seizures following viral infection. *J Virol* **85**, 6913–6922 (2011).
37. Lanser, M. E. & Brown, G. E. Stimulation of rat hepatocyte fibronectin production by monocyte-conditioned medium is due to interleukin 6. *J Exp Med* **170**, 1781–1786 (1989).
38. Beezhold, D. H., Leftwich, J. A. & Hall, R. E. P48 induces tumor necrosis factor and IL-1 secretion by human monocytes. *J Immunol* **143**, 3217–3221 (1989).
39. te Velde, A. A., Huijbens, R. J., Heije, K., de Vries, J. E. & Figdor, C. G. Interleukin-4 (IL-4) inhibits secretion of IL-1 beta, tumor necrosis factor alpha, and IL-6 by human monocytes. *Blood* **76**, 1392–1397 (1990).
40. Schroder, J. M., Persoon, N. L. & Christophers, E. Lipopolysaccharide-stimulated human monocytes secrete, apart from neutrophil-activating peptide 1/interleukin 8, a second neutrophil-activating protein. NH2-terminal amino acid sequence identity with melanoma growth stimulatory activity. *J Exp Med* **171**, 1091–1100 (1990).
41. Hosking, M. P. & Lane, T. E. The role of chemokines during viral infection of the CNS. *PLoS Pathog* **6**, e1000937 (2010).

42. Hosking, M. P., Liu, L., Ransohoff, R. M. & Lane, T. E. A protective role for ELR+ chemokines during acute viral encephalomyelitis. *PLoS Pathog* **5**, e1000648 (2009).
43. Carpentier, P. A., Getts, M. T. & Miller, S. D. Pro-inflammatory functions of astrocytes correlate with viral clearance and strain-dependent protection from TMEV-induced demyelinating disease. *Virology* **375**, 24–36 (2008).
44. Jin, Y. H. *et al.* Differential virus replication, cytokine production, and antigen-presenting function by microglia from susceptible and resistant mice infected with Theiler's virus. *J Virol* **81**, 11690–11702 (2007).
45. Lipton, H. L. & Dal Canto, M. C. Chronic neurologic disease in Theiler's virus infection of SJL/J mice. *J Neurol Sci* **30**, 201–207 (1976).
46. Lipton, H. L. & Melvold, R. Genetic analysis of susceptibility to Theiler's virus-induced demyelinating disease in mice. *J Immunol* **132**, 1821–1825 (1984).
47. Brinton, M. A. & Nathanson, N. Genetic determinants of virus susceptibility: epidemiologic implications of murine models. *Epidemiol Rev* **3**, 115–139 (1981).
48. Ingersoll, M. A., Platt, A. M., Potteaux, S. & Randolph, G. J. Monocyte trafficking in acute and chronic inflammation. *Trends Immunol* **32**, 470–477 (2011).
49. Ransohoff, R. M. Microglia and monocytes: 'tis plain the twain meet in the brain. *Nat Neurosci* **14**, 1098–1100 (2011).
50. Shi, C. & Pamer, E. G. Monocyte recruitment during infection and inflammation. *Nat Rev Immunol* **11**, 762–774 (2011).
51. Silva, M. T. When two is better than one: macrophages and neutrophils work in concert in innate immunity as complementary and cooperative partners of a myeloid phagocyte system. *J Leukoc Biol* **87**, 93–106 (2010).
52. Soehnlein, O. & Lindbom, L. Phagocyte partnership during the onset and resolution of inflammation. *Nat Rev Immunol* **10**, 427–439 (2010).
53. Deb, C. & Howe, C. L. NKG2D contributes to efficient clearance of picornavirus from the acutely infected murine brain. *J Neurovirol* **14**, 261–266 (2008).
54. Shapiro, S. S. & Wilk, M. B. An Analysis of Variance Test for Normality (Complete Samples). *Biometrika* **52**, 591–611 (1965).
55. Sidak, Z. Rectangular Confidence Regions for the Means of Multivariate Normal Distributions. *J Am Stat Assoc* **62**, 626–633 (1967).
56. Curran-Everett, D. & Benos, D. J. Guidelines for reporting statistics in journals published by the American Physiological Society: the sequel. *Adv Physiol Educ* **31**, 295–298 (2007).
57. Kruskal, W. H. & Wallis, W. A. Use of Ranks in One-Criterion Variance Analysis. *J Am Stat Assoc* **47**, 583–621 (1952).
58. Dunn, O. J. Multiple comparisons using rank sums. *Technometrics* **6**, 241–252 (1964).

Acknowledgments

This work was supported by grant NS64571 from the NIH/NINDS and by a generous gift from Donald and Frances Herdrich. Dr. Allan Bieber provided expert help with the bone marrow transplant experiments.

Author contributions

CLH conceived, designed, and analyzed all experiments, wrote the manuscript, and performed the histopathology, pathology scoring, viral titer, and cell isolations. RLC performed the flow cytometry, bone marrow transplants, and adoptive transfers. RSS performed the histopathology. BMS and SJL performed the behavioral analyses. EJB participated in the early design of the project and performed the TUNEL analysis. WFS assisted in experimental design, data analysis, and preparation of the manuscript.

Additional information

Supplementary information accompanies this paper at http://www.nature.com/scientificreports

Competing financial interests: The authors declare no competing financial interests.

How to cite this article: Howe, C.L. *et al.* Hippocampal protection in mice with an attenuated inflammatory monocyte response to acute CNS picornavirus infection. *Sci. Rep.* **2**, 545; DOI:10.1038/srep00545 (2012).